



Characterization of displaced bipolar cells in the tiger salamander retina

Bruce R. Maple, Jian Zhang, Ji-Jie Pang, Fan Gao, Samuel M. Wu *

Cullen Eye Institute, Baylor College of Medicine, One Baylor Plaza, Mail Station NC-205, Houston, TX 77030, USA

Received 21 August 2004; received in revised form 27 September 2004

Abstract

In immunocytochemical studies of the tiger salamander retina, 17% of neurons in the outer nuclear layer did not label for recoverin, a photoreceptor marker. Lucifer yellow injection showed a population of cells in the ONL to be displaced bipolar cells, with axon terminals that stratified exclusively in the OFF sublamina of the inner plexiform layer (IPL), and predominately within the cone-dominated region of the OFF sublamina. Glutamate generated a dendritic cationic conductance increase in all displaced bipolar cells tested, and typical cone-dominated bipolar cell light responses were observed among displaced cells that stratified in the central IPL. We conclude that displaced bipolar cells in the tiger salamander retina are entirely OFF-center cells, and predominately cone-dominated cells.

© 2004 Elsevier Ltd. All rights reserved.

Keywords: Displaced bipolar cells; Outer nuclear layer; Retina; Salamander

1. Introduction

Bipolar cells of the vertebrate retina integrate visual signals from photoreceptors, and they transmit signals to the IPL, where visual information is segregated among third order neurons. The axons of salamander bipolar cells give rise to fine telodendria, which ramify laterally at one or more distinct strata within the IPL. Because different types of bipolar cells synapse at different depths within the IPL, a mapping of visual information is created along the depth of the IPL. Parameters mapped in this way include the polarity (ON or OFF receptive field center) and spectral nature (rod and cone components) of the visual stimulus. Among vertebrate retinas in general, OFF bipolar cells (which hyperpolarize in response to illumination of the receptive field cen-

ter) tend to make output synapses in the distal IPL, while ON bipolar cells (which depolarize in response to central illumination) tend to synapse in the proximal IPL (Euler, Schneider, & Wässle, 1996; Famiglietti, Kaneko, & Tachibana, 1977; Famiglietti & Kolb, 1976; Kolb, 1979; Maple & Wu, 1996; Wu, Gao, & Maple, 2000). Also, across vertebrate species, rod-dominated ON bipolar cells send axons to the proximal margin of the IPL (Cajal, 1893; Kolb, 1970; Wu et al., 2000). Salamander retinas also possess rod-dominated OFF bipolar cells that make output synapses near the distal margin of the IPL (Maple, Gao, & Wu, 1999). Thus, in salamander retinas, rod signals are sent primarily to the margins of the IPL, while cone signals are sent primarily to the central IPL (Wu et al., 2000).

Previously, we have categorized salamander bipolar cells according to axonal morphology (Wu et al., 2000), since this relates directly to their role in the processing of visual information in the IPL. Bipolar cells vary greatly with respect to other morphological characteristics, however, most notably the position of their cell

* Corresponding author. Tel.: +1 713 798 5966; fax: +1 713 798 6457.

E-mail address: swu@bcm.tmc.edu (S.M. Wu).

bodies within the retina. While in all vertebrates the somas of most bipolar cells are situated within the inner nuclear layer (INL), bipolar cells with somas lying in the outer nuclear layer (ONL) have been observed in a number of species. Such “displaced” bipolar cells have been described in teleost, amphibian, reptilian, and mammalian retinas (Cajal, 1893; Dogiel, 1891). In fact, displaced bipolar cells account for about one third of the somas in the ONL of some turtle retinas (Kouyama & Ohtsuka, 1985). In this study we compared the axon morphologies of displaced bipolar cells with those of the more common “INL” bipolar cells in the tiger salamander retina. The responses of displaced bipolar cells to light stimuli and to dendritic application of glutamate were also examined. Finally, the density of displaced bipolar cells in the ONL was compared to the estimated density of bipolar cells in the INL.

2. Materials and methods

2.1. Experimental animals

Larval tiger salamanders (*Ambystoma tigrinum*) purchased from Charles D. Sullivan Co. (Nashville, TN) and Kon's Direct, Inc. (Germantown, WI) were used in this study. All animals were handled in accordance with the guidelines of Baylor College of Medicine and the National Institutes of Health. The salamanders were anesthetized with MS-222, then decapitated, and the eyes were enucleated.

2.2. Immunocytochemistry

Retinas were fixed in 4% paraformaldehyde in phosphate-buffered saline (PBS; pH 7.4) for 30–60 min at room temperature, and then extensively rinsed with PBS. Wholemound retinal tissue was blocked with 3% donkey serum in PBS with 0.5% Triton X-100 and 0.1% sodium azide from 2 h to overnight to reduce non-specific labeling. The tissue was then incubated in primary antibody in the presence of 1% donkey serum/PBS with 0.5% Triton X-100/0.1% sodium azide for 3–10 days at 4°C. Controls lacking primary antibodies were blank. After extensive washing with PBS containing 0.5% Triton X-100/0.1% sodium azide the tissue was incubated overnight with immunofluorescent secondary antibody. After further rinsing the tissue was mounted with Vectrashield. The specimens were then observed with a confocal laser-scanning microscope (Zeiss LSM510). Stacked images were acquired through the whole retina, using Zeiss LSM-PC software, and cells were counted manually.

Rabbit polyclonal bovine recoverin antibody was kindly provided by Dr. A.M. Dizhoor (Pennsylvania College of Optometry, Elkins Park, PA), and used in a

dilution of 1:1000. Rabbit polyclonal anti-glutamate and guinea pig polyclonal anti-GABA were obtained from Chemicon International (Temecula, CA) and used in a dilution of 1:1000. Secondary antibodies were donkey conjugated CY3 (Jackson ImmunoResearch, West Grove, PA) and Alexa 488 (Molecular Probes), used in a dilution of 1:100. TOPRO3 (0.01 µl/ml), a nuclear dye used to label cell bodies in ONL, was obtained from Molecular Probes (Eugene, OR).

2.3. Electrophysiology

The procedures for retinal slicing were described in previous publications (Werblin, 1978; Wu, 1987). For dark-adapted experiments, dissection and recording were done under infrared illumination with a dual Nitemare infrared scope (BE Meyers, Redmond, WA). Retinal slices were continuously superfused with a Ringer's solution containing 108 mM NaCl, 2.5 mM KCl, 1 mM MgCl₂, 2 mM CaCl₂, and 5 mM Hepes (adjusted to pH 7.7). In some experiments involving glutamate application, 2 mM CoCl₂ was substituted for 2 mM CaCl₂, in order to suppress synaptic transmission. Bipolar cells were voltage-clamped with pipets of about 5 MΩ resistance. The pipets were filled with Cs-containing solutions with a chloride concentration set to yield a chloride equilibrium potential of −50 mV or −60 mV (Maple et al., 1999), and a correction of 9.5 mV or 10 mV, respectively, was applied to correct for the liquid junction potential at the tip of the patch pipet prior to seal formation. No series resistance compensation was used in these experiments, but the series resistance was carefully monitored during recording and maintained at a level less than 20 MΩ.

The pipets also contained 4 mM Lucifer yellow, which was used to characterize cell morphology via fluorescence microscopy. Morphometric measurements were made using an eyepiece micrometer. The level at which axonal processes stratified in the IPL was characterized by the distance from the processes to the distal margin of the IPL. This distance was expressed in inner plexiform units (IPU), where the thickness of the entire IPL was defined as 1.0 IPU. Also, the position of the bipolar cell soma within the depth of the retina was characterized by the distance from the distal margin of the IPL to the base of the soma. This distance was expressed in inner nuclear units (INU), where 1.0 INU corresponded to the entire thickness of the INL.

Glutamate was applied to bipolar cell dendrites by pressure ejection from pipets with a lumen of about 1 µm. A photostimulator was used to deliver 500–600 µm diameter spots of light to the retina via a microscope epi-illuminator. Light intensity was controlled with neutral density filters, and was measured in log units of attenuation. The intensity of unattenuated (log *I* = 0) 500 nm light (determined with a radiometric detector) was 2.05×10^7 photons µm^{−2} s^{−1}.

3. Results

3.1. The ONL of the salamander retina contains a high density of displaced bipolar cells

Fig. 1A shows a fluorescence micrograph of a transverse section of salamander retina that was double-immunolabeled with glutamate and GABA antibodies. Glutamate labeling (red) was apparent in both rods and cones within the ONL, and it was particularly strong in bipolar cells, mostly situated within the distal INL. Also labeling for glutamate were a number of small ONL cells situated near the cone somata, but lacking the inner and outer segments typical of cones. Some of these cells possessed an unmistakable Landolt club (as in the cell marked a), typical of bipolar cells. Others lacked such a pronounced club, but possessed a small apical swelling (as the cell marked b). GABA labeling (green) was apparent in the INL, but not in the ONL. These results suggest that glutamatergic neurons other than photoreceptors are present in the ONL of the salamander retina.

Immunolabeling for recoverin, a photoreceptor marker, also suggested the presence of non-photoreceptor cells in the ONL. Fig. 1B shows the ONL of a retina that was labelled with recoverin antibody (green) and counterstained with the nuclear dye TOPRO3 (blue). As reported previously, the rods were weakly labeled by recoverin antibody, and the cones strongly immunolabeled (Zhang, Yang, & Wu, 2004). In addition the nuclei of some cells that did not stain for recoverin were visible along the proximal margin of the ONL. Fig. 1C illustrates a confocal image of a whole mount retina stained in this manner. This optical section of the proximal

Table 1

Mean densities of cells in the ONL of the salamander retina

	Rods	Cones	Recoverin-negative nuclei
Cells/mm ² ± s.d.	4400 ± 1134	3526 ± 908	1630 ± 420
Percentage of ONL nuclei	46	37	17

These were derived from nuclei counts for six flatmount retinas.

ONL shows numerous recoverin-negative nuclei interspersed among a lattice of strongly labeled cones. Imaging the ONL at different depths, a count of ONL nuclei was performed for three retinas, and the mean density of rods, cones, and recoverin-negative nuclei in the midperiphery was determined (Table 1). It was determined that 17% of all nuclei in the ONL belonged to recoverin-negative cells, or cells that were probably not photoreceptors.

When patching clamping ONL cells in retinal slices with Lucifer yellow-filled electrodes, in almost all cases cells with non-photoreceptor morphology displayed the morphology of bipolar cells, i.e., they had dendrites within the OPL and axons that coursed into the IPL. These axons gave rise to telodendria that stratified at one or two levels of the IPL. Examples of such monostatified and bistratified bipolar cells are shown in Fig. 2A and B, respectively. During the course of this study, only one ONL cell displayed a morphology characteristic of horizontal cells, so displaced horizontal cells probably comprise only a very small fraction of the recoverin-negative ONL cells. We concluded that close to 17% of the cells in the ONL of the tiger salamander retina are bipolar cells.

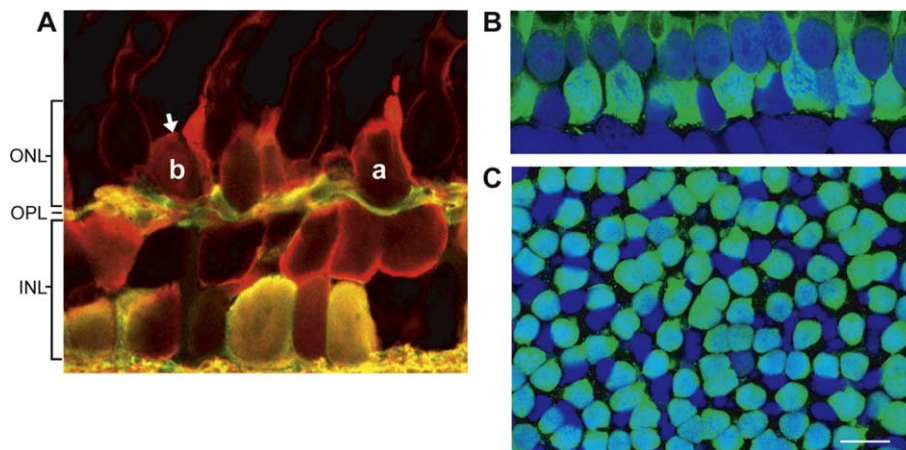


Fig. 1. (A) Glutamate (red) and GABA (green) immunoreactivity in the distal retina. Glutamate-positive cells lacking outer segments are visible in the ONL, along the margin of the OPL. These cells typically display a Landolt club (a) or small apical swelling (b, arrow). (B) Recoverin immunoreactivity in the ONL (green). Nuclei are counterstained with TOPRO3 (blue). The row of deep blue nuclei at the top of the photograph belong to rod photoreceptors. Below this lies the layer of cone somata, which are highly recoverin immunoreactive. Recoverin-negative cells (blue) are visible adjacent to the cone somata. (C) A mosaic of photoreceptors and recoverin-negative nuclei imaged at the level of the cone somata. Counts of rods, cones, and recoverin-negative ONL cells were made from a series of such images. Scale bar = 20 μ m.

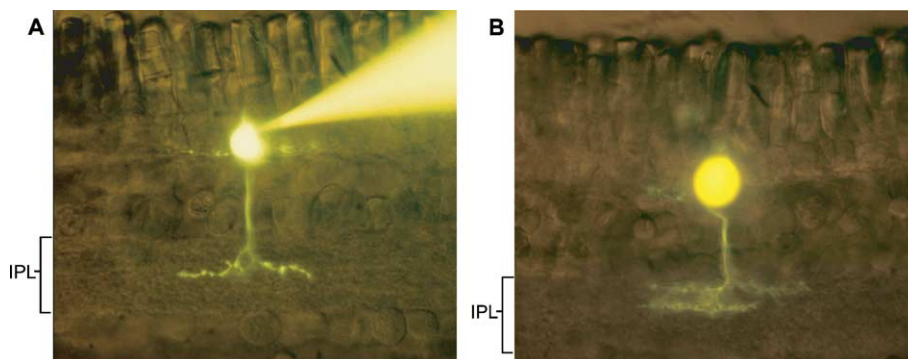


Fig. 2. Lucifer yellow filled displaced bipolar cells. The axons of these cells stratified in the OFF sublamina of the IPL (0.0–0.55IPU). (A) A monostratified cell, with telodendria ramifying within the central IPL. (B) A bistratified cell, with telodendria stratified at two distinct levels of the IPL.

The somas of these “displaced” bipolar cells were often not confined exclusively to the ONL. Frequently they spanned the OPL and extended somewhat into the INL. Fig. 3 illustrates the distribution of soma positions observed for a population of 236 Lucifer yellow filled bipolar cells that were morphometrically characterized. This histogram gives the level of the base of the soma in the INL, expressed as a fractional distance from the proximal margin of the INL. In other words, a cell with base position at 1.0INU was a completely displaced cell, one that did not extend into the INL at all. The bipolar cells varied greatly with respect to size and shape, so this simple measure did not completely characterize their depth within the retina. The distribution was clearly bimodal, however. In practice, cells at depths of 0.8–1.0INU had somas situated more in the ONL than in the INL, and these cells formed a popula-

tion distinctly different from the INL bipolar cells situated at 0.1–0.7INU. In subsequent discussion we will refer to the 0.8–1.0INU cells as *displaced* bipolar cells.

3.2. The axons of displaced bipolar cells terminate exclusively in the OFF lamina of the IPL, and predominately in the cone-dominated strata

The bipolar cells represented in the histogram of Fig. 3 were also characterized with respect to the level(s) at which their telodendria ramified within the IPL. Fig. 4A gives a scatter plot showing the soma position and level of IPL stratification for each of 195 monostratified bipolar cells (panel a). All of the displaced cells in this plot stratified within the region of 0.0–0.55IPU, which has been previously characterized as the OFF sublamina of the salamander IPL (Maple & Wu, 1996; Wu et al., 2000). Most of the displaced monostratified cells fell into a cluster with stratification ranging from 0.32 to 0.55IPU, a region corresponding to the cone-dominated OFF strata (Maple et al., 1999; Wu et al., 2000). Although two displaced bipolar cells stratified in the distal 3/10 of the IPL (the rod-dominated OFF strata), clearly the vast majority (94%) of monostratified displaced bipolar cells projected to the cone-dominated OFF strata.

Fig. 4A also gives the mean level of the soma base for four regions of IPL stratification (panel b). The bipolar cells that stratified at 0.32–0.55IPU, on average, had the most distally situated somas, due largely to the fact that displaced cells comprised such a large percentage (77%) of this group. Interestingly, despite the low percentage (<6%) of displaced cells among the cells stratifying in the region of 0.0–0.32IPU, the mean soma position for these cells was significantly distal to the mean position for cells ramifying in the ON sublamina (0.55–1.0IPU). In fact, even when the displaced bipolar cells were excluded, the somas of the OFF bipolar cells were situated more distally ($.49 \pm .02$ INU (s.e.)) than the somas of the ON bipolar cells ($.41 \pm .02$ INU). It is

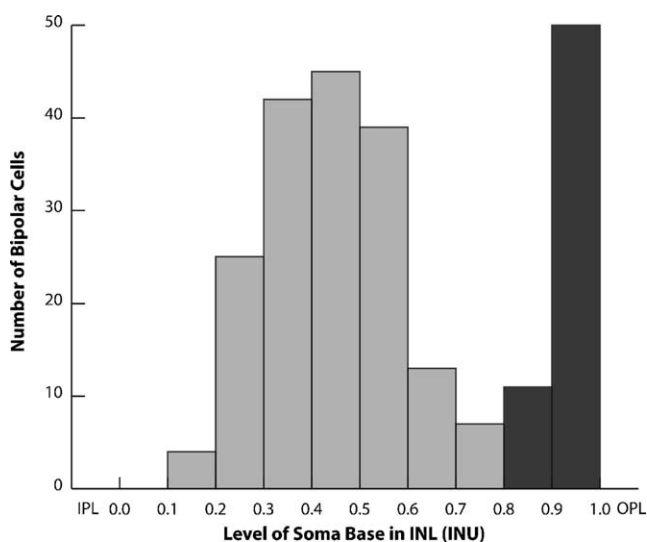


Fig. 3. The distribution of bipolar cell somas along the depth of the INL. This histogram shows the position of the base of the soma for 236 Lucifer yellow filled bipolar cells. The distribution is clearly bimodal, with the displaced bipolar cells corresponding to cells with somas positioned at 0.8–1.0INU.

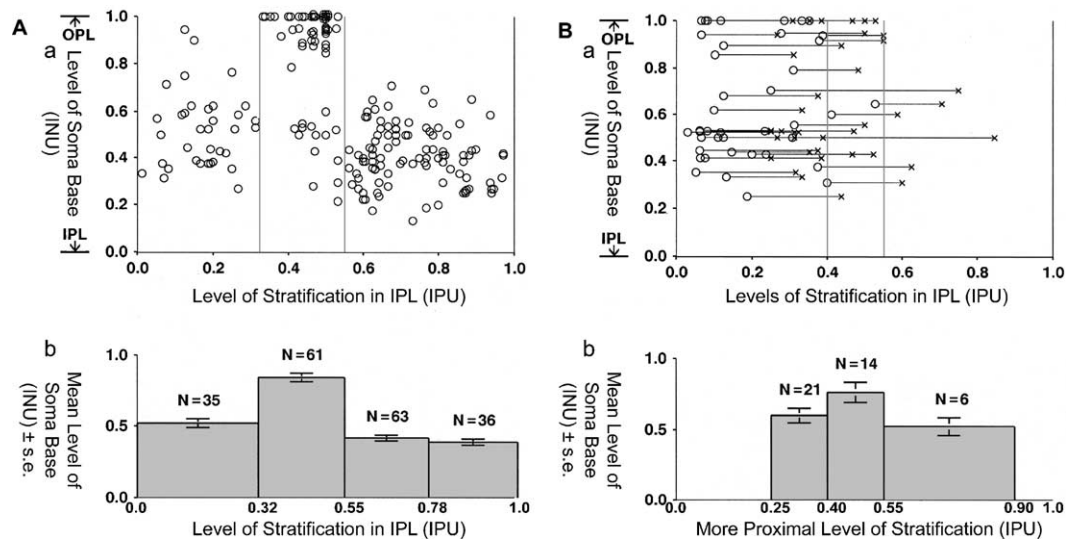


Fig. 4. Soma depth vs. level of stratification in the IPL. (A) A scatter plot for 195 monostratified bipolar cells that were filled with Lucifer yellow (a). The left margin of the plot represents the border between the IPL and INL (0.0 IPU), and the right margin of the plot represents the border between the IPL and ganglion cell layer (1.0 IPU). Most displaced cells (0.8–1.0 INU) stratified in the central IPL (0.32–0.55 IPU). The mean soma depth (\pm s.e.) for each of four IPL regions is given in (b). The somas of OFF cells, on average, were situated more distally than the somas of ON cells. (B) A scatter plot for 41 bistratified bipolar cells (a). For each cell the level of the distal stratum is given by a circle, and the level of the proximal stratum is given by an X. A histogram of mean soma depth (\pm s.e.), binned according to the level of the proximal stratum is given in (b). The three bins correspond to distally-bistratified OFF, centrally-bistratified OFF, and bistratified ON/OFF cells.

important to note, however, that while the difference between these means is significant, it is small compared to the standard deviations for these distributions.

The telodendria of the bistratified displaced bipolar cells also ramified exclusively in the OFF sublamina of the IPL (Fig. 4B). Like their INL counterparts, these cells exhibited a wide range of axonal morphologies. The more distal telodendria of the bistratified displaced cells stratified at a level ranging from 0.06 to 0.38 IPU, while their more proximal telodendria stratified at a level ranging from 0.25 to 0.55 IPU. A similar range of morphologies was observed among INL bipolar cells, but in addition there were some INL bipolar cells with proximal telodendria ramifying in the ON sublamina. Such trans-sublamina cells appear to have both ON and OFF characteristics (Pang, Gao, & Wu, 2004; Wu et al., 2000).

We have previously classified the INL bistratified OFF bipolar cells into two broad groups, based on the level of stratification of their more proximal telodendria. In general these cells are intermediate with respect to the

relative strengths of rod and cone input, but those with proximal telodendria that stratify more distally (0.25–0.40 IPU) are relatively rod-dominated, while those with proximal telodendria that stratify more centrally (0.40–0.55 IPU) are relatively cone-dominated (Wu et al., 2000). Panel b of Fig. 4B shows that the more centrally-stratifying bistratified OFF cells have somas situated more distally, on average, than bistratified cells in the more distally-stratifying class. This reflects a higher percentage of displaced somas among the centrally-bistratified cells (57%) than among the distally-bistratified cells (24%).

Table 2 breaks the OFF bipolar cells down into four classes, and summarizes the relative frequency with which these classes were encountered among the displaced bipolar cells and among the INL bipolar cells. Strikingly different distributions are apparent for the displaced cells and INL cells. While centrally-monostratified and centrally-bistratified cells accounted for 89% of the displaced bipolar cells, they represented only 29% of the OFF bipolar cells with somas in the INL.

Table 2

A breakdown of displaced bipolar cells and OFF INL bipolar cells into four morphological classes

	Distally-monostratified (0.0–0.32 IPU)	Distally-bistratified (0.25–0.40 IPU) ^a	Centrally-bistratified (0.40–0.55 IPU) ^a	Centrally-monostratified (0.32–0.55 IPU)
Percentage of displaced cells	3	8	13	76
Percentage of OFF INL cells	48	23	9	20

^a The bistratified cells are categorized according to their more proximal level of stratification.

3.3. The physiological properties of displaced bipolar cells, like those of INL bipolar cells, are correlated with the level of axon termination

Fig. 5A illustrates responses of a displaced bipolar cell to focal pressure ejection of 200 μ M glutamate at the cell's dendrites. The cell was bathed in cobalt Ringer's solution, in order to suppress any synaptic transmission that might otherwise be induced by the stimulus. 100 ms pulses of glutamate were delivered for holding potentials ranging from -70 to $+40$ mV. An I/V curve for the peaks of these responses is shown in Fig. 5B. Interpolation between the responses at -10 mV and 0 mV yielded an estimate of -5.0 mV for the reversal potential of the response, indicating that glutamate elicited a cationic conductance increase in this cell. In all of the displaced bipolar cells examined (two distally-monstratified, 33 centrally-monstratified, and seven bistratified cells) glutamate induced a cationic conductance increase at the dendrites. Among the six displaced cells for which the reversal potential of the glutamate response was carefully measured in cobalt Ringer's solution, the mean value was -6.3 ± 2.1 mV (s.d.), close to the value of -4.7 ± 3.4 mV previously reported for OFF bipolar cells in the salamander retina (Maple & Wu, 1996). We conclude that all displaced bipolar cells in the salamander retina possess dendritic glutamate receptors capable of generating an OFF light response.

Fig. 6A and B illustrate light responses for a centrally-monstratified displaced bipolar cell and bistratified displaced bipolar cell, respectively. These responses (panel b) were typical of light responses observed previously for cone-dominated OFF bipolar cells with somas situated in the INL (Maple et al., 1999; Wu et al., 2000). The responses to light onset were small (as in Fig. 6B) or dominated by a chloride conductance increase generated by amacrine cell synapses (Fig. 6A). The responses at light offset were biphasic,

consisting of a rapid, transient conductance increase that reversed near 0 mV, followed by a slower conductance increase that reversed near E_{Cl} . The rapid component was generated by photoreceptor synapses, and it reflects an increase of glutamate release from photoreceptors as they depolarized following termination of the light stimulus. The slower component represents inhibitory input from amacrine cells at the IPL. Consistent with the results of glutamate application experiments, the cells of Fig. 6A and B were OFF bipolar cells. Their photoreceptor inputs were mediated by sign conserving synapses, so glutamate activated a cationic conductance increase in these cells. These findings are also consistent with the results of an earlier study which found OFF-center responses for both of two displaced salamander bipolar cells examined (Hare, Lowe, & Owen, 1986).

These cells were also characterized with respect to spectral sensitivity using the spectral difference method (Yang & Wu, 1996). Responses to 500 nm and 700 nm stimuli were recorded with the holding potential set at E_{Cl} . A "spectral difference" ($\Delta S = S_{700} - S_{500}$) was calculated for each cell, where S_{700} and S_{500} corresponded to intensities of 700 nm and 500 nm light that yielded responses equal in amplitude, for a small criterion amplitude. This gave a measure of rod or cone dominance, since ΔS is about $3.4 \log$ units for rods and about $0.1 \log$ units for cones (Yang & Wu, 1990). Matched 500 nm and 700 nm light responses for the displaced cells of Fig. 6 are shown in panels (c) and (d), respectively. The value of ΔS for the centrally monstratified cell in Fig. 6A was $0.8 \log$ units (0.87 ± 0.4 , $N = 3$), indicating that it was strongly cone-dominated. This fell within a range of ΔS values ($0.9 \pm 0.3 \log$ units) previously reported for INL bipolar cells with similar axon morphologies (Maple et al., 1999). The displaced bistratified bipolar cell of Fig. 6B was also cone-dominated ($\Delta S = 0.7 \log$ units) (0.89 ± 0.37 , $N = 5$). In general,

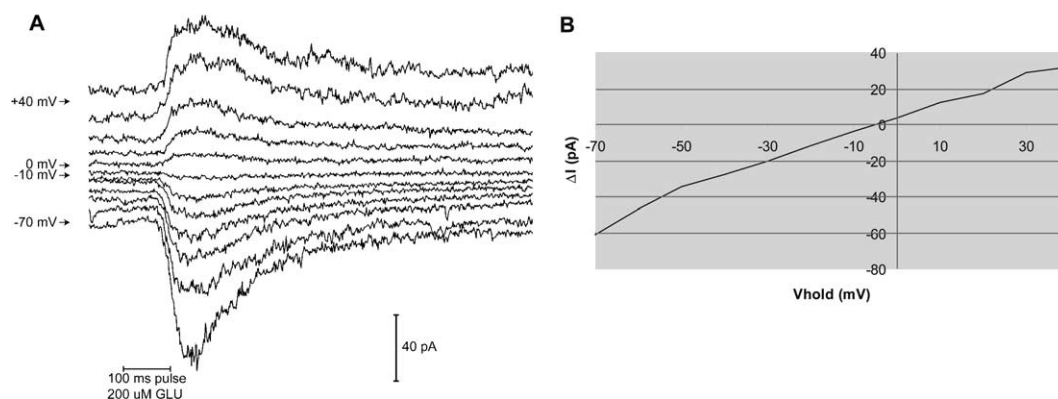


Fig. 5. Dendritic glutamate responses of a displaced bipolar cell (monstratified at 0.5 IPU) under voltage clamp. (A) A set of responses to 100 ms puffs of 200 μ M L-glutamate, for holding potentials ranging from -70 mV to $+40$ mV. (B) An I/V curve for the peak of the glutamate response, derived from the average of two responses at each potential. The interpolated reversal potential for the response was -5.0 mV.

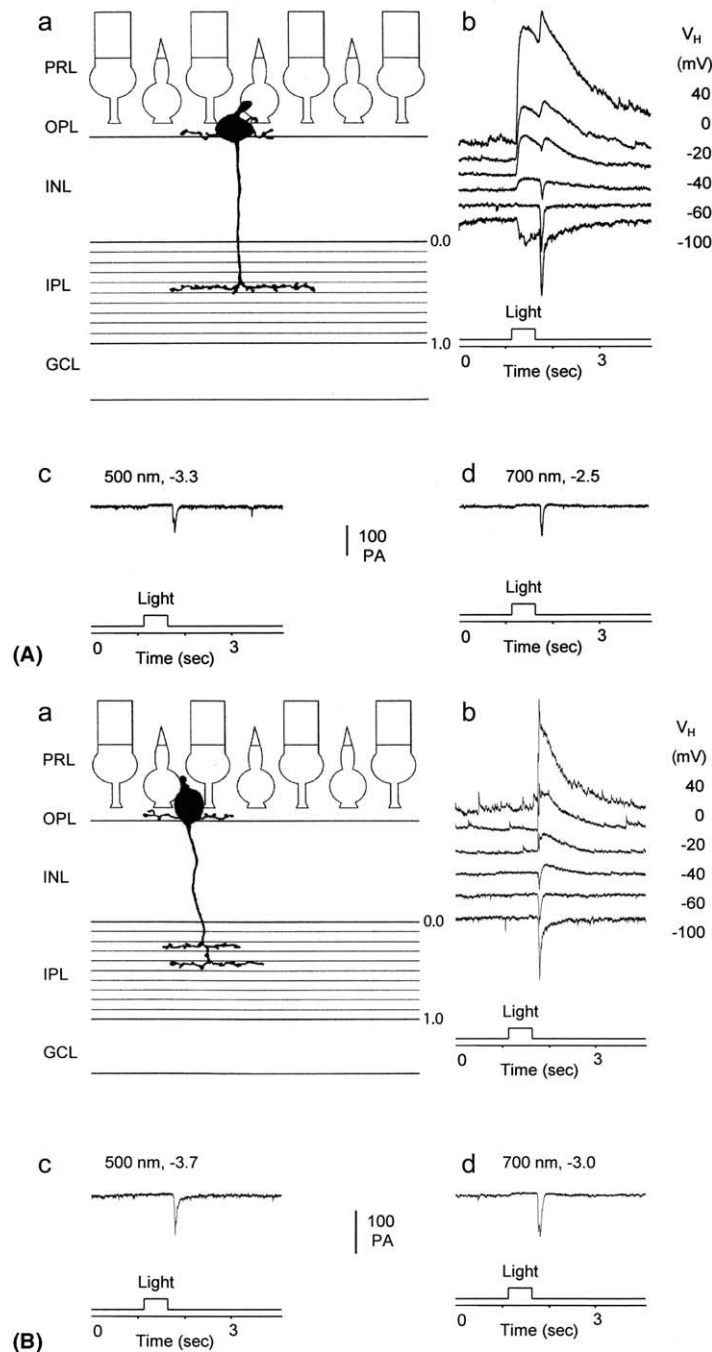


Fig. 6. Light responses of displaced bipolar cells. (A) A sketch of a centrally monostratified bipolar cell (a); light responses of this cell at various holding potentials (V_H) (b); matched light responses at E_{Cl} (-60 mV) are shown for 500 nm (c) and 700 nm (d) stimuli. The stimulus intensities for these responses (-3.3 and -2.5 log units, respectively) yielded a spectral difference of 0.8 log units. (B) A sketch of a centrally bistratified bipolar cell (a); light responses of this cell at various holding potentials (b); matched light responses for 500 nm (c) and 700 nm (d) stimuli yielded a spectral difference of 0.7 log units.

bistratified OFF bipolar cells display a wide range of morphologies and a considerable range of ΔS values, but ΔS for the bistratified displaced cell of Fig. 6B fell within the range (0.9 ± 0.2 log units) previously reported for bistratified INL bipolar cells with a proximal stratum at 0.45 – 0.55 IPU (Wu et al., 2000).

We have not performed light response experiments for the relatively rare distally-monostratified displaced bipolar cells. However, in these cells we have observed spontaneous large-amplitude miniature excitatory post-synaptic currents typical of the rod-dominated INL bipolar cells that stratify in the distal $1/4$ of the IPL

(Maple, Werblin, & Wu, 1994). In summary, the physiological properties of displaced bipolar cells appear to be similar to those of INL bipolar cells with the similar axon morphologies.

4. Discussion

We have estimated that displaced bipolar cells represent about 17% of the somas in the ONL of the tiger salamander retina. This value is considerably larger than a previously reported estimate of 7.3% (Sherry, 2003). The earlier estimate was based on the assumption that all bipolar cells were labeled by calretinin antibodies. In fact, not all bipolar cells are calretinin immunoreactive (Zhang & Wu, unpublished observations), so this assumption would be expected to lead to an underestimate of the density of displaced bipolar cells.

In any case, it is evident that a sizable fraction of OFF bipolar cells in the salamander retina have displaced somas. Displaced bipolar cells constituted 45% of the Lucifer yellow-filled OFF bipolar cells described in this study. This percentage, however, is likely biased by whether the experimenter selected for ONL or INL somas. We estimate that the tiger salamander retina has a mean density of 1630 displaced bipolar cells/mm², but since no specific immunochemical marker has been found for OFF bipolar cells, we have no direct means for determining the density of these cells in the INL. Markers do exist, however, for the other major cell types, so we can roughly estimate the density of INL OFF bipolar cells by subtracting the density of cells that are not OFF bipolar cells from the total density of nuclei in the distal and middle INL (about 7800 cells/mm² in the midperiphery (Zhang & Wu, 2003)). A large majority of ON bipolar cells in the salamander retina (3198 cells/mm²) are immunoreactive for the alpha subunit of G-protein G_0 , and it has been estimated that the rod-dominated ON bipolar cells, which are $G_{0\alpha}$ -negative, account for another 702 cells/mm² (Zhang & Wu, 2003). It has also been estimated that GABAergic and glycinergic amacrine cells account for a combined mean density of about 200 cells/mm² in the middle INL (Zhang et al., 2004). In addition the densities of horizontal cells and Muller cells have been estimated at 545 cells/mm² and 1389 cells/mm², respectively (Zhang & Wu, unpublished data). Subtracting the sum of the densities for these subpopulations from the total density of 7800 cells/mm² in the distal and middle INL gives an estimate of 1966 INL cells/mm² that are likely to be OFF bipolar cells. Interestingly, the sum of this value plus the estimated density of *displaced* OFF bipolar cells (a total of 3596 cells/mm²) is close to the mean density of ON bipolar cells (3900 cells/mm²). Furthermore, this analysis suggests that displaced bipolar

cells constitute about 45% of all OFF bipolar cells in the tiger salamander retina, a value nearly identical to the ratio observed in our electrophysiological experiments.

In a recent study that correlated the light response attributes and axonal morphologies of over 200 INL bipolar cells, far fewer OFF cells were monostратified in the central strata (0.3–0.55 IPU) than in the distal strata (0–0.3 IPU) of the IPL (Pang et al., 2004, Fig. 1). Centrally monostратified OFF bipolar cells were evidently under-represented in this study, because their somas reside mostly in the ONL. However, the few INL OFF bipolar cells that did stratify in the central IPL exhibited light responses very similar to those described here for displaced bipolar cells with similar axon morphologies, i.e., the responses were cone-dominated, with large transient inward currents at light offset (Pang et al., 2004; Figs. 2, 4 and Table 1). The characteristics of bipolar cell light responses appear to correlate closely with the level of axon terminal stratification, regardless of the depth of the soma within the retina.

As we have not observed any physiological differences between displaced bipolar cells and INL bipolar cells with similar IPL stratification, our conclusion that displaced bipolar cells are predominantly cone-dominated OFF-center cells may have more relevance for retinal development than for retinal circuitry. Little is known about the developmental mechanisms that direct the stratification of bipolar cell axonal processes in the IPL and the migration of some bipolar cell somas to the INL. In a developmental sense, bipolar cells and photoreceptors appear to be closely related. Both are glutamatergic neurons that differentiate relatively late in retinal development (Raedler & Sievers, 1975). Furthermore, photoreceptors transiently project axons to the IPL prior to formation of the OPL (Johnson, Williams, Cusato, & Reese, 1999). Perhaps with respect to some developmental factors the displaced bipolar cells are more akin to photoreceptors than to the INL bipolar cells. It should also be noted that even among the INL bipolar cells, some developmental mechanism apparently causes the somas of ON-center cells, on average, to migrate more proximally than the OFF-center cells. These findings point to a need for further research into the mechanisms of retinal development.

Acknowledgments

We thank Dr. A.M. Dizhoor for providing the antibody to recoverin and Dr. Roy Jacoby for critically reading this manuscript. This work was supported by grants from the NIH (EY 04446), NIH Vision Core (EY 02520), the Retina Research Foundation (Houston), and Research to Prevent Blindness, Inc.

References

- Cajal, S. R. (1893). La rétine des vertébrés. *La Cellule*, 9, 17–257.
- Dogiel, A. S. (1891). Ueber die nervösen Elemente in der Retina des Menschen. *Arch Mikr Anat*, 44, 622–648.
- Euler, T., Schneider, H., & Wässle, H. (1996). Glutamate responses of bipolar cells in a slice preparation of the rat retina. *Journal of Neuroscience*, 16, 2934–2944.
- Famiglietti, E. V., Jr., Kaneko, A., & Tachibana, M. (1977). Neuronal architecture of on and off pathways to ganglion cells in carp retina. *Science*, 19, 1267–1269.
- Famiglietti, E. V., Jr., & Kolb, H. (1976). Structural basis for ON- and OFF-center responses in retinal ganglion cells. *Science*, 194, 193–195.
- Hare, W. A., Lowe, J. S., & Owen, G. (1986). Morphology of physically identified bipolar cells in the retina of the tiger salamander, *Ambystoma tigrinum*. *Journal of Comparative Neurology*, 252, 130–138.
- Johnson, P. T., Williams, R. R., Cusato, K., & Reese, B. E. (1999). Rods and cones project to the inner nuclear layer during development. *Journal of Comparative Neurology*, 414, 1–12.
- Kolb, H. (1970). The organization of the outer plexiform layer of the primate retina: electron microscopy of Golgi-impregnated cells. *Philosophical Transactions of the Royal Society of London Series B—Biological Sciences*, 258, 261–283.
- Kolb, H. (1979). The inner plexiform layer of the cat: electron microscopic observations. *Journal of Neurocytology*, 8, 295–329.
- Kouyama, N., & Ohtsuka, T. (1985). Quantitative morphological study of the outer nuclear layer in the turtle retina. *Brain Research*, 345, 200–203.
- Maple, B. R., Werblin, F. S., & Wu, S. M. (1994). Miniature excitatory postsynaptic currents in bipolar cells of the tiger salamander retina. *Vision Research*, 34, 2357–2362.
- Maple, B. R., & Wu, S. M. (1996). Synaptic inputs mediating bipolar cell responses in the tiger salamander retina. *Vision Research*, 36, 4015–4023.
- Maple, B. R., Gao, F., & Wu, S. M. (1999). Glutamate receptors differ in rod- and cone-dominated off-center bipolar cells. *NeuroReport*, 10, 3605–3610.
- Pang, J. J., Gao, F., & Wu, S. M. (2004). Stratum-by-stratum projection of light response attributes by retinal bipolar cells of *Ambystoma*. *Journal of Physiology*, 558, 249–262.
- Raedler, A., & Sievers, J. (1975). The development of the visual system of the albino rat. *Advances in Anatomy Embryology and Cell Biology*, 50(3), 1–88.
- Sherry, D. (2003). Neurochemical heterogeneity of retinal bipolar cells. *Optometry*, 74, 422–429.
- Werblin, F. S. (1978). Transmission along and between rods in the tiger salamander retina. *Journal of Physiology*, 28, 449–470.
- Wu, S. M. (1987). Synaptic connections between neurons in living slices of the larval tiger salamander. *Journal of Neuroscience Methods*, 20, 139–149.
- Wu, S. M., Gao, F., & Maple, B. R. (2000). Functional architecture of synapses in the inner retina: segregation of visual signals by stratification of bipolar cell axon terminals. *Journal of Neuroscience*, 20, 4462–4470.
- Yang, X. L., & Wu, S. M. (1990). Synaptic inputs from rods and cones to horizontal cells in the tiger salamander retina. *Science in China B*, 33, 946–954.
- Yang, X. L., & Wu, S. M. (1996). Response sensitivity and voltage gain of the rod- and cone-horizontal cell synapses in dark- and light-adapted tiger salamander retina. *Journal of Neurophysiology*, 76, 3863–3874.
- Zhang, J., & Wu, S. M. (2003). G₀₂ Labels ON bipolar cells in the tiger salamander retina. *Journal of Comparative Neurology*, 416, 276–289.
- Zhang, J., Yang, Z., & Wu, S. M. (2004). Immunocytochemical analysis of spatial organization of photoreceptors and amacrine and ganglion cells in the tiger salamander retina. *Visual Neuroscience*, 21, 1–10.